 CMC, vol.2, no.3, pp.163-176, 2005

An FEM study on crack tip blunting in ductile fracture initiation

N. Ramakrishnan [1] **and P. Rama Rao** [2]

Abstract: Ductile fracture is initiated by void nucleation at a *characteristic distance* (l_c) from the crack tip and propagated by void growth followed by coalescence with the tip. The earlier concepts expressed l_c in terms of grain size or inter-particle distance because grain and particle boundaries form potential sites for void nucleation. However, Srinivas et al. (1994) observed nucleation of such voids even inside the crack tip grains in a nominally particle free Armco iron. In an attempt to achieve a unified understanding of these observations, typical crack-tip blunting prior to ductile fracture in a standard C(T) specimen (Mode I) was studied using a finite element method (FEM) supporting large elasto-plastic deformation and material rotation. Using a set of experimental data on Armco iron specimens of different grain sizes, it is shown that none of the locations of the maxima of the parameters stress, strain and strain energy density correspond to l_c. Nevertheless, the size of the zone of intense plastic deformation, as calculated from the strain energy density distribution ahead of the crack tip in the crack plane, compares well with the experimentally measured l_c. The integral of the strain energy density variation from the crack tip to the location of void nucleation is found to be linearly proportional to J_{IC}. Using this result, an expression is arrived at relating l_c to $J_{IC}$and further extended to $CTOD_c$.

keyword: Ductile fracture, finite element method, fracture toughness, characteristic length.

Notation

$CTOD_C$	critical crack tip opening displacement
E	Young's modulus
J_{IC}	critical fracture toughness
K	strength parameter appearing in power law (Eqn. 4)
l_c	characteristic distance
l_u	unloading distance ahead of the crack tip
m	a material coefficient used in equation (Eqn. 3) relating J_{IC} and $CTOD_C$
n	strain hardening exponent
r	distance from the crack tip
ε	effective strain
ε^*	critical strain used in equation (Eqn. 2)
ε_c	critical strain for void nucleation
ϕ	strain energy density variation ahead of the crack tip
ϕ_c	critical strain energy density for void nucleation (Eqn. 5)
κ	a constant appearing in equation (Eqn. 7)
σ	a strength parameter used in equation (Eqn. 3) relating J_{IC} and $CTOD_C$
σ_o, σ_y	yield strength
σ_f	flow strength
σ_u	ultimate strength
σ^*	an integral stress measure (as in Eqn. 11)

1 Introduction

Several studies have shown that ductile fracture of metallic materials is preceded by void nucleation at a distance from the crack tip. The voids then grow, coalesce with the crack tip and initiate the fracture process. The distance from the crack tip at which a void of this type is formed is termed the 'characteristic-distance' [Ritchie and Thompson (1985)]. Nucleation of these voids is generally attributed to the presence of second phase particles or grain boundaries [Ritchie and Thompson (1985); Green et al. (1976); Knott (1980); Lin et al. (1986); Garrison Jr. (1984)] in the vicinity of the crack tip and therefore the 'characteristic distance' has been conjectured to be an integral multiple of the inter-particle distance or the grain size**,** as the case may be. This led the earlier investigators to explain initiation of ductile fracture as a threshold effect of a critical stress as well as strain developing over a distance from the crack tip. It can also be viewed as the void nucleation zone or intense deformation zone around the crack tip, designated as the process

[1] Regional Research Laboratory, Hoshangabad Road, Bhopal- 462 026, India.

[2] International Advanced Research Centre for Powder Metallurgy and New Materials, Balapur P. O., Hyderabad – 500 005, India.

zone in the earlier studies by [Garrison Jr. (1984); Srinivas et al. (1994)], subjected to a limiting deformation energy for initiation of the fracture.

According to the 'critical *CTOD* criterion' by Rice et al. (1970) ductile fracture occurs when void sites are first enveloped by a region of intense strain at the crack tip. Here, the J$-l_c$ relationship is given as

$$J_{IC} = \sigma_0 l_c \tag{1}$$

where l_c is assumed to be roughly equal to $CTOD_C$ itself and J_{IC} to be proportional to the yield strength (σ_0). A modified version of this relationship proposed by Ritchie and Thompson (1985) referred to as the 'stress modified critical strain criterion', is expressed as,

$$J_{IC} = \sigma_0 \varepsilon^* l_c \tag{2}$$

where a critical strain (ε^*) term is introduced. Equation 2, where J_{IC} is considered proportional to the product of strength and a critical strain, implies that initiation of ductile fracture takes place when the local plastic strain energy density exceeds $\sigma_0 \varepsilon^*$ over a characteristic distance l_c.

Hancock (1980, 1992) considers such a 'structure-dictated characteristic distance' to be applicable only to what he refers to as 'dirty materials' that contain a significant volume fraction of void nucleating inclusions and inhomogeneities. In 'clean' materials, his concept is that the crack tip strain state dictates the magnitude of the characteristic distance. He substantiates his viewpoint with the observations related to slip induced voids. Interestingly, Srinivas et al. (1994) in their experimental study on a relatively 'clean' particle-free Armco iron, observed voids even inside the crack-tip grains. This observation, like those reported by Wilsdorf (1983) on a pure metal single crystal failing by ductile fracture, showed that the presence of particles or grain boundaries is not a pre-requisite for this type of void nucleation. This was a motivation for the present work aimed at studying how the crack tip stress distribution in a 'clean' continuum varies as a function of yield strength and strain hardening exponent, and also to study the $J - l_c$ relationship to understand the significance of the characteristic distance l_c, keeping in view the following questions:

1. Has the 'characteristic distance' any physical meaning or is it merely a useful adjustable length parameter since J is dimensionally equivalent to the product of any energy density or a strength term, and a length term?

2. If l_c bears physical significance, does it depend on the microstructure or the stress and the strain distributions as well? In other words, is l_c influenced by structure alone or mechanics as well?

3. Is l_c experimentally observable in a similar way to stretch zone width? If so, how is J_{IC} related to l_c?

Finite element calculations (FEM) have been performed to find answers to these questions. Several engineering disciplines use FEM successfully and its utility in fracture mechanics is well known. FEM has been used to investigate the stress and strain distributions in the vicinity of cracks for elastic-plastic constitutive behaviour and to determine the fracture parameters, *J* and *CTOD*. Crack-tip blunting involves very large deformations, that is, large strain and extensive material rotation. It is, therefore, essential that the FEM that is used for simulating crack-tip blunting should be based on a large deformation framework. The present work uses a special finite deformation algorithm developed by Ramakrishnan et al. (1999), which has been tested and validated in metal forming applications where the deformation is analogous to that of crack tip blunting. The validation procedure employed to ascertain the applicability of this algorithm to the present case is presented in section 2.

Rice (1968) proposed the concept of path independent J-integral and several related experimental and analytical studies ensued. Notable one is the analytical representation of *J* as well as *CTOD* using HRR field equations [Hutchinson (1968a,b); Rice and Rosengren (1968)] describing the elastic-plastic stress and strain distribution at the crack tip. J_{IC} characterises the material's threshold crack tip stress and strain for initiation of ductile fracture and $CTOD_C$ quantifies the extent of crack tip blunting as given by Begley et al. (1972) and Landes et al. (1972). Analytical considerations [Rice (1968); Rice et al. (1968); Shih (1981)] led to the relationship between J_{IC} and $CTOD_C$,

$$J_{IC} = m \sigma CTOD_C \tag{3}$$

where σ is a stress-measure and m is understood to be a material constant.

The present study attempts achieving an insight into l_c using a large deformation FEM and develop $J_{IC} - l_C$ - $CTOD_C$ relationships. In the FEM analysis, the crack tip zone is treated as a homogeneous continuum. Introduction of voids, particles and grain boundaries in the FEM model such as cases given in [Gao et al. (1998); Gullerud et al. (2000)] is deliberately avoided in order to specifically understand the pure continuum behaviour. The experimentally obtained properties of Armco iron by Srinivas et al. (1972) for different grain sizes are used as the effective properties of the homogeneous continuum. The study essentially pertains to ductile crack initiation and has not concerned with crack growth related aspects. Further, FEM analysis is used more as a numerical experiment to understand the earlier experimental results of Srinivas et al. (1972). Therefore the specimen geometry, the material properties and the boundary conditions were so chosen as to conform to the experimental conditions. This would allow validation of the numerical study as well. The experimental measurements of fracture toughness of ductile Armco iron made by Srinivas et al. (1972) were in terms of J_{IC} as defined by the ASTM standards. The present numerical study accordingly addresses only J_{IC} and did not look at T-stress parameter [Tvergaard (1994); Jackson et al (2004)] or propagation [Tchouikov et al (2004)].

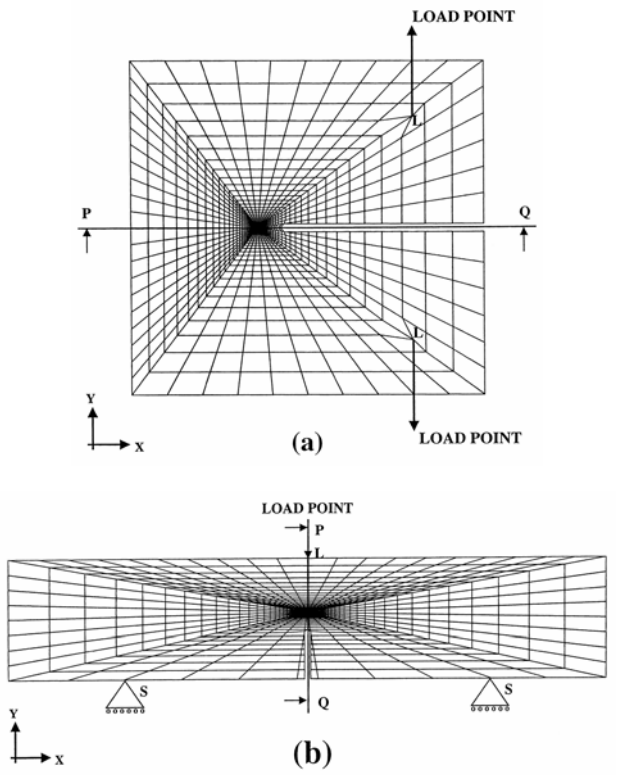

Figure 1 : Finite element mesh model (a) Compact tension specimen, and b) Single edge bend specimen.

2 Numerical simulation

2.1 The FEM model

The investigation is limited to planar analysis of compact tension specimen (C (T)) subjected to mode-I type of loading. For the purpose of validating the numerical procedure, the single edge cracked bend specimen (SE (B)) geometry was also considered but the investigation does not include any analysis of the deformation in SE (B). The FEM mesh models of the C(T) and the SE (B) of ASTM E 813-81(1986) are shown in Figures 1a and 1b respectively. The symmetry in these cases permits consideration of only one half of the specimen geometry for computational economy.

In a review paper, Liebowitz & Moyer (1989) cite various investigators successfully employing dense mesh with conventional elements and advocate against the use of singular or special crack tip elements unless required specifically. Following the above guidelines, the mesh was constructed with a set of bi-linear four-noded quadrilateral elements. Since the experimentally measured l_c is about 100 microns [Srinivas et al. (1994)], the size of the crack tip element was chosen to be about 5 microns and increased radially in geometric progression (in order to reduce the size difference of the neighbouring elements, arithmetic progression was also attempted but was found to be computationally uneconomical) as suggested by Tsamasphyros & Glannakopoulos (1989). This type of mesh configuration allows the study of deformation at the microscopic scale in the vicinity of the crack tip as well as the global load-displacement variation for the entire specimen. Here, about 10 to 15 elements are accommodated within a distance of about 100 microns from the crack tip in the initial state and more in the deformed state due to the Poisson's contraction. A magnified view of the mesh morphology around the crack tip is shown in Figure 2a and that of the corresponding deformed mesh in Figure 2b.

l_c is measured in the deformed state. Use of smaller crack tip elements did not improve the convergence sig-

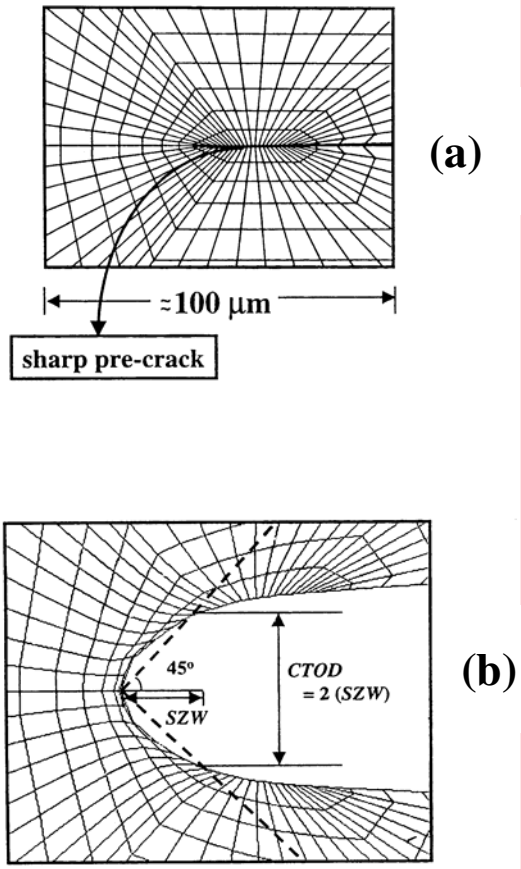

Figure 2 : Magnified view of the FEM mesh at the crack tip (a) Initial configuration, and (b) Deformed configuration.

nificantly. Further, in lower hardening cases, it caused computational difficulties due to severe mesh distortions arising due to the steep variation of the crack tip plastic strain. Varying the total number of elements from 500 to 2000 and examining the convergence of the numerical results, an optimum of 1300 elements was arrived at. Also, comparing an unstructured FE mesh model with the structured one, keeping the element size distribution near the crack tip similar, the difference in the results was found to be negligible. Therefore, only the structured mesh was used in all the numerical simulations for the post processing-convenience it offers.

In the case of the C(T) geometry, the nodes falling on the symmetry line PQ (Figure 1a) are arrested in the Y-direction and the load point L is constrained in the X-direction. The load is applied in steps of Y-directional displacements at node L. For the SE (B), the nodes on the line PQ (Figure 1b) are arrested in the X-direction and the support point node S in the Y-direction. The load is applied in steps of Y-directional displacements at node L. As measured in the actual experiment, a critical load point displacement of 1.5 mm, with respect to the symmetry plane, was applied and the corresponding deformation contours were used for the analysis.

The material undergoes a large strain and rotation at the crack tip, which necessitates a constitutive framework based on finite deformation for the numerical simulation. Accordingly the present investigation uses a finite deformation algorithm developed by Ramakrishnan et al. (1999) based on total elastic incremental plastic strain (TEIP strain) that was originally developed for simulating metal forming processes. The flow behaviour of the material is assumed to follow the power - law

$$\sigma_f = K\varepsilon^n \tag{4}$$

where $\sigma_f$is the true flow stress, K is the strength coefficient, ε is the elasto-plastic strain and n is the strain hardening exponent. The present study does not consider the influence of strain-rate or temperature.

The investigation essentially comprises a number of FEM simulations. The numerical data were obtained in the form of stress, strain or similar parameter distributions given the material properties and the load-line displacements. The FEM analysis includes the determination of J and CTOD. *CTOD* was measured using the 45^o line method [McMeeking (1997) and Tracey (1976)] as shown in Figure 2b. The value of J was determined using the load vs. load-line displacement variation given in ASTM [E813-81 (1986) & E1152-87 (1987)] and was verified using the line integral approach given by Maguid (1989). It is known that mode I type fracture in a C(T) specimen of highly ductile materials does not conform to plane strain condition. In this regard Schmitt & Hollstein's (1985) proposal of averaging the results of the plane strain and plane stress conditions was found to be simple and attractive in numerically reproducing the experimental results with reasonable accuracy. All the results presented in this investigation were obtained using this averaging procedure.

2.2 Validation

The general aspects of the large deformation algorithm have since been validated with a number of analytical and

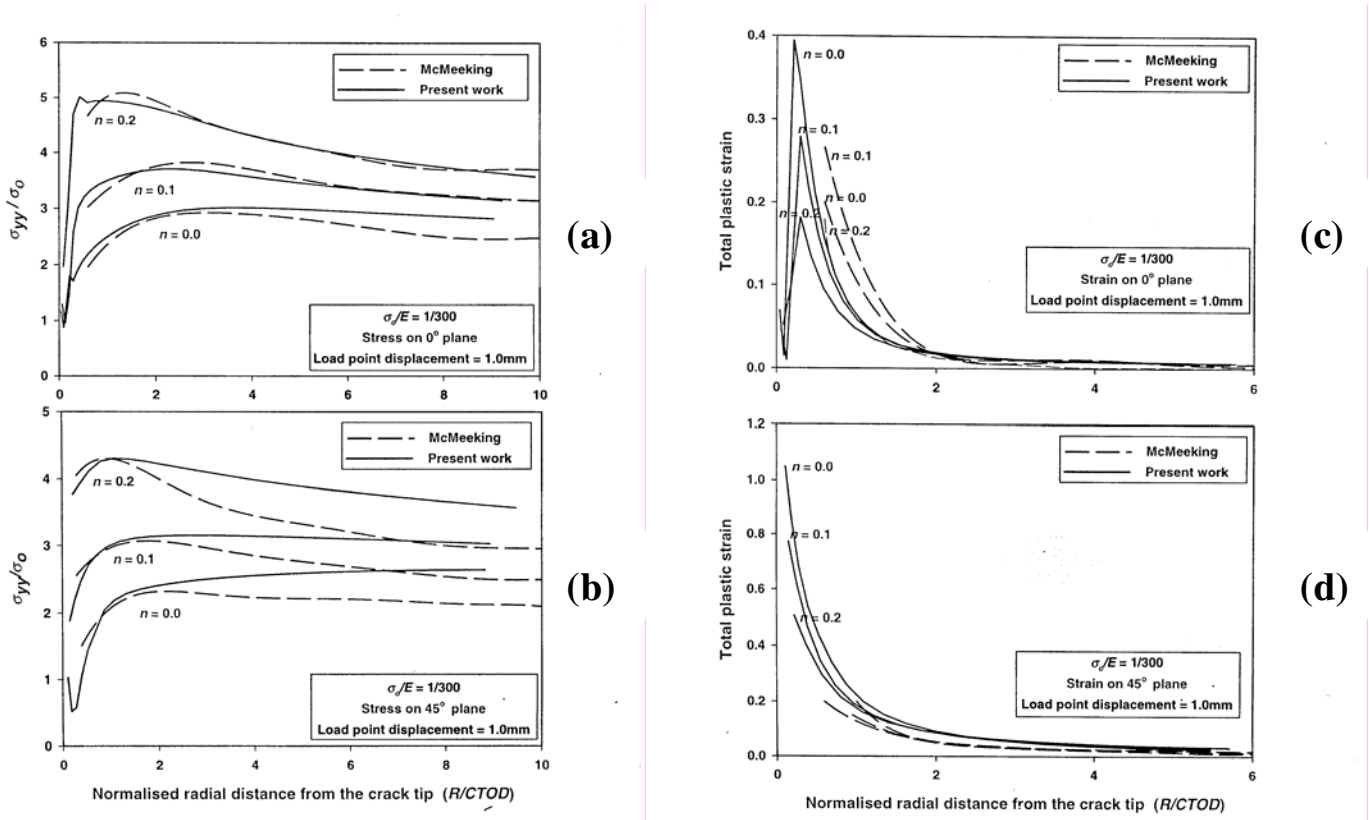

Figure 3 : Comparison of the results of the present work with those of McMeeking (1977) (a) stress in 0^o plane, (b) stress in 45^o plane, (c) plastic strain in 0^oplane, and (d) plastic strain in 45^o plane.

experimental data in the earlier work of Ramakrishnan et al. (1999), validation specific to the present investigation was carried out with reference to the published numerical [McMeeking (1977)] and the experimental results [Srinivas et al. (1994)].

The correctness of the procedure for computing J and CTOD was confirmed by comparing the results (J and CTOD) obtained for the ASTM [E813-81 (1986) & E1152-87 (1987)] specified C (T) and the SE (B). The results, as expected, were nearly independent of the specimen type. Then the focus was on the verification of the crack tip stress-strain distribution using the published data of McMeeking (1977) who performed a large deformation FEM analysis of crack-tip blunting for small scale yielding of a power-law hardening material. He employed a circular mesh model around a blunt notch and imposed the displacements of the elastic crack-tip singular field at the circular boundary for plane strain conditions. The normalised crack tip stress (σ_{yy}/σ_0) as a function of the normalised radial distance from the crack tip (*R/CTOD*) and the normalised plastic strain with the same abscissa, obtained by McMeeking (1977) are compared with those of the present study in Figure 3. In all these cases, σ_0/E was taken as 1/300 and n as 0.0, 0.1 and 0.2 as was reported in McMeeking (1977). The comparison of the stress distributions pertaining to 0^o plane is shown in Figure 3a and that for the 45^o plane in Figure 3b. Similarly, the plastic strain variations are compared in Figures 3c and 3d.

While the 0^o plane stress distribution agrees well with that of McMeeking (1977), the 45^o plane stress variation shows a noticeable deviation. While 0° plane experiences little material rotation, the 45° plane undergoes a large rotation. The deviation can be attributed to the difference in the way the material rotation is modelled in these two studies. McMeecking's model employs 'Jaumann rate' which implicitly assumes Sin $\theta = \theta$ while the large deformation model of the present study makes no such assumption. In the case of plastic strains, the present study shows a sharp dip close to the crack tip due

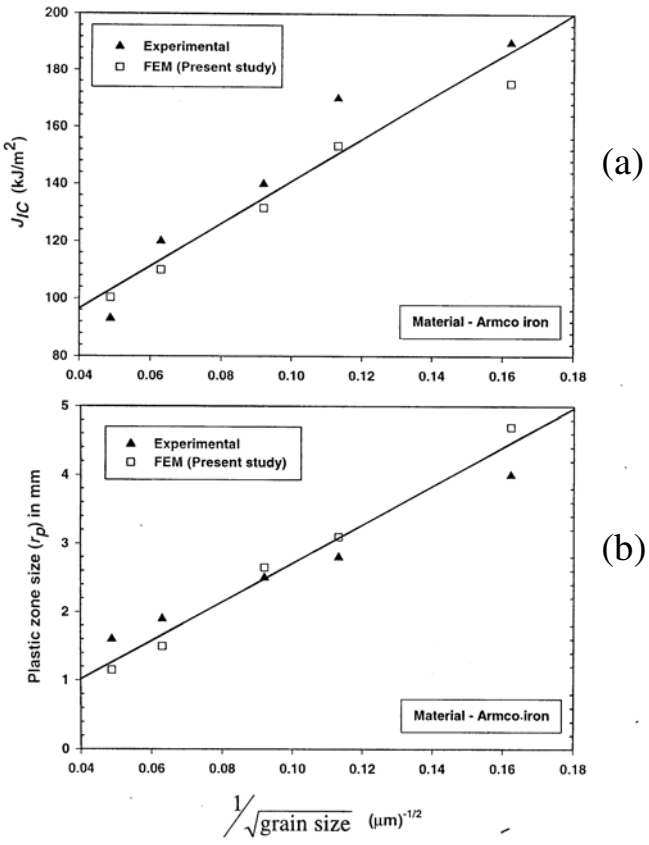

Figure 4 : Experimental validation of the numerical procedure (a) comparison of the computed J_IC with the experimental data [Srinivas et al. (1994)], and (b) comparison of the computed plastic zone size with the experimental data [Srinivas et al. (1991)].

to large blunting and the corresponding stress relaxation. This aspect is not reflected in McMeeking (1977), which could be due to the assumption of small-scale yielding and the difference in the mesh discretisation.

In Figure 4a, experimentally measured J_{IC} values of Armco iron by Srinivas et al (1994) corresponding to grain sizes 38, 78, 118, 252, 420 microns, are compared with the present numerical results and the agreement is satisfactory. The strength coefficient (K) and the strain- hardening exponent (n) for Armco iron of the various grain sizes, tabulated in Srinivas et al. (1991) were used as 'material input data' for validating the FEM results. No assumption was made regarding the relationship between the grain size and the yield strength. Figure 4b shows a reasonable matching of the experimentally [Srinivas et al. (1991)] obtained plastic zone sizes (r_p) and the numerically determined ones. Here, the plastic zone is delineated based on where the effective stress exceeds the yield strength and its size was measured as the extent of the plastic zone perpendicular to the crack tip. Since the 2D cross-sectional view of the plastic zone is not a circular one, measuring the dimension of the zone perpendicular to the crack plane standardizes it and this aspect has been discussed in Srinivas et al. (1991).

3 FEM analysis of Characteristic distance (l_C)

FEM simulations were performed to find the correspondence, if any, between l_c and the different types of stress and strain distributions in the vicinity of the crack tip during blunting. The variations of the plastic strain, the strain energy density and the instability parameter were also studied. The FEM results were then compared with the experimental data of Srinivas et al. (1994) to select the most suitable correlation.

3.1 Stress, strain, energy distributions

The variation of σ_{yy} and the hydrostatic stress (σ_m), both normalised with σ_0, as a function of the radial distance from the crack tip (r) for a set of representative values of σ_0 / E and n are presented in Figures 5a & 5b and in each case for 0^o, 30^o and 60^o planes. In this exercise, for the purpose of illustration, a load-point displacement of 1.5 mm was imposed as reported in Srinivas et al. (1994). It can be observed that the variation shows relatively sharp maxima for high strain hardening cases and diffused ones for near zero-hardening cases indicating a well marked void nucleation region for higher 'n' materials compared to that for the lower 'n' ones. In the case of both σ_{yy} and σ_m, the locations of maximum do not provide a measure of l_c .

More specifically, corresponding to the experimental load-line displacements of Srinivas et al. (1994), the FEM stress distributions for Armco iron were computed. The maxima of the parameter distributions did not correlate with the observed characteristic distances and at best only the order of magnitude of the distances of the maximum stress location from the crack tip matched the experimental l_c. Further, while the experimental trend indicates an increasing l_c with increasing strain hardening exponent, the distances of the maxima from the crack tip decrease with increasing strain hardening exponent.

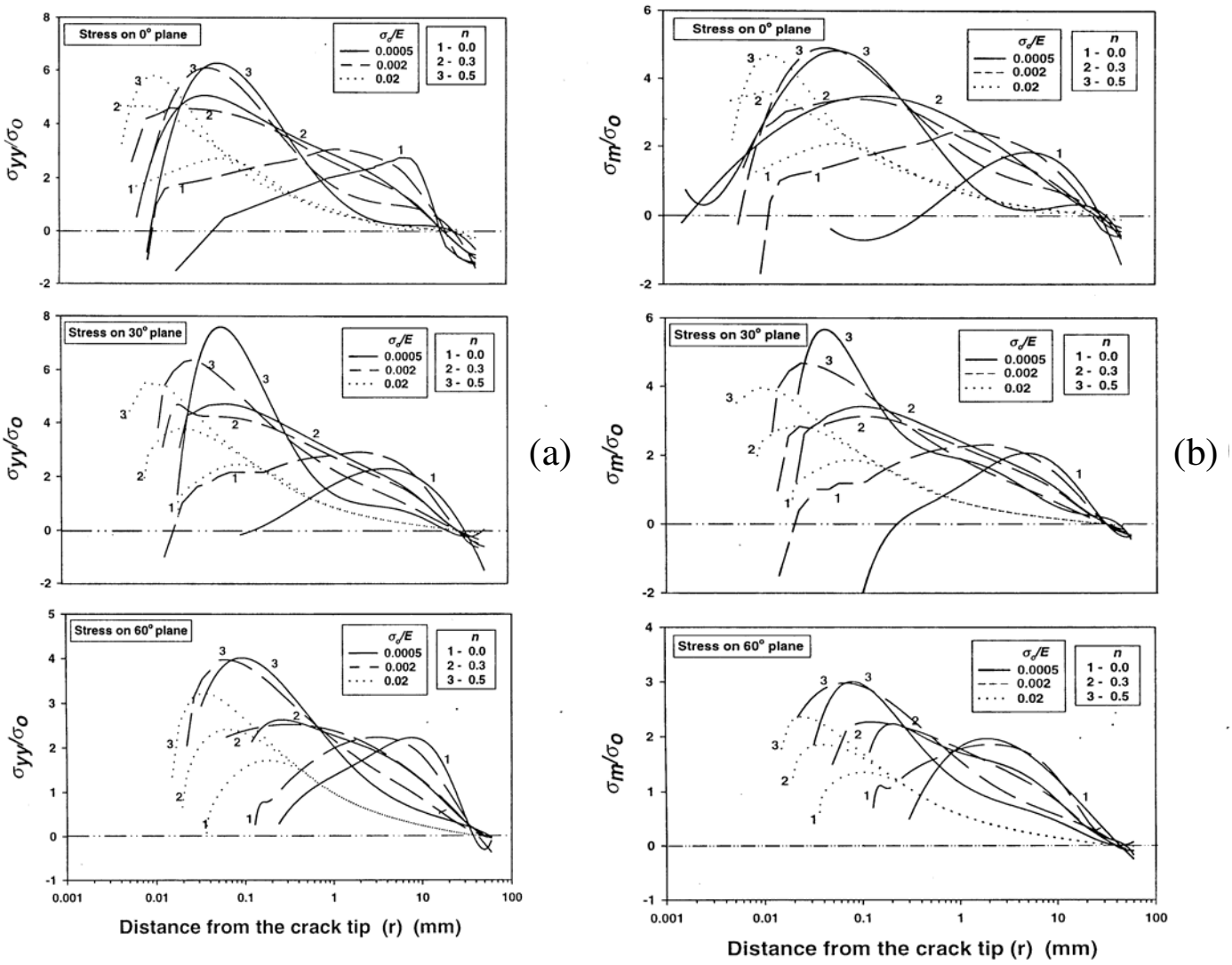

Figure 5 : Stress distribution around the crack tip (a) σ_{yy} / σ_0, and (b) hydrostatic stress (σ_m / σ_0)

An unstable zone is observed around the crack tip as shown in Figures 6a & 6b. The extent of instability was computed based on a parameter suggested by Ortiz, Leroy and Needleman (1987), which essentially characterises planar discontinuity in strain field. This OLN [Ortiz, Leroy & Needleman (1987)] parameter was used successfully in capturing certain shear instabilities, by Ramakrishnan and Atluri (1994a,b), where smaller values of the parameter correspond to higher instability. Figures 6a & 6b present the variation of OLN parameter pertaining to Armco iron with load-line displacement and grain size respectively. In Figure 6a the grain size is varied for a given load-line displacement and vice versa in Figure 6b. Although the instability around the crack tip occurs at a finite distance from the crack tip, these distances are much smaller than the corresponding experimentally [Srinivas et al. (1994)] obtained l_c values and therefore explain only the voids formed almost at the crack tip but not the ones formed away from it. In addition, it can be seen in Figure 6a that the minima of OLN values turn out to be nearly independent of grain size and thus the strain hardening exponent which is not the case with the experimentally determined characteristic distances.

The variation of the plastic strain energy density as a function of the radial distance from the crack tip for a set of extreme values of σ_0 / E and n are shown in Figure 7. Finite maximum values can be seen only in cases pertaining to crack tip unloading. Even in these cases, the

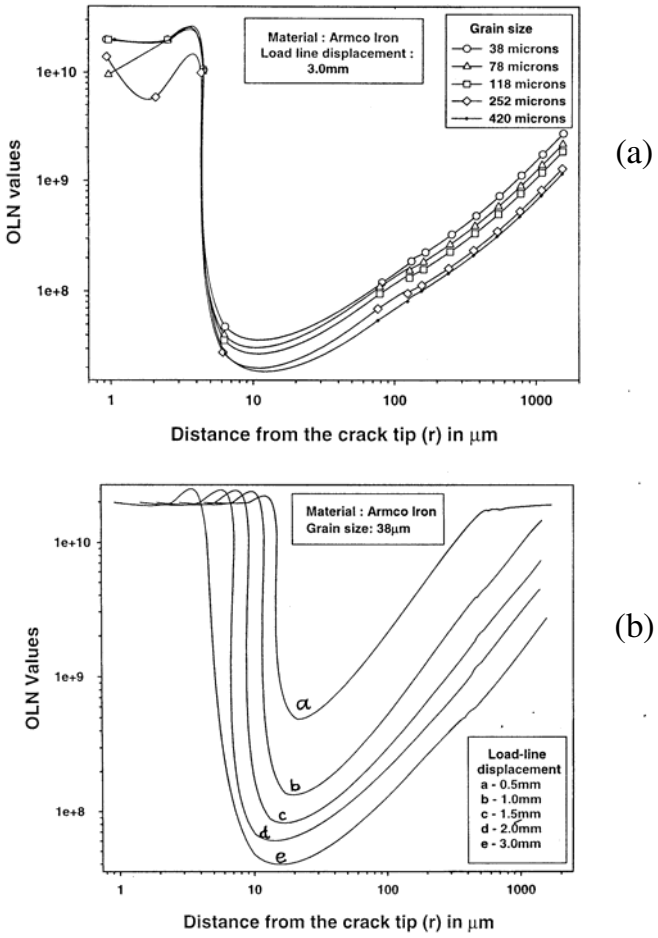

Figure 6 : Instability at the crack tip: variation of OLN parameter for different (a) grain sizes, and (b) load-line displacements

distances of the maximum from the crack tip do not correspond to the 'distances' of our interest. This supports the earlier deduction that the instability-induced voids formed very close to the crack tip in the 0^o plane are not related to the 'characteristic distance'. In Figure 7, although the location of the maximum does not correlate with the characteristic distance, the plastic deformation is found to be intense in a zone, the size of which roughly matches with the characteristic distance. That is, although the plastic deformation spreads up to about 1000 microns, pronounced deformation is limited to a zone of about 100 to 200 microns only. Therefore, a detailed analysis of the zone of intense plastic deformation was carried out. It was then found that l_c can indeed be predicted with reasonable accuracy and its dependence on grain size matched the experimentally observed trend. The results are discussed in the following sections.

3.2 Determination of l_c

A methodology to determine l_c will be first presented using the distribution of strain energy density (ϕ) and then its experimental validation using the data on Armco iron as in Srinivas et al. (1994).

The variation of ϕ on the crack plane for Armco iron of

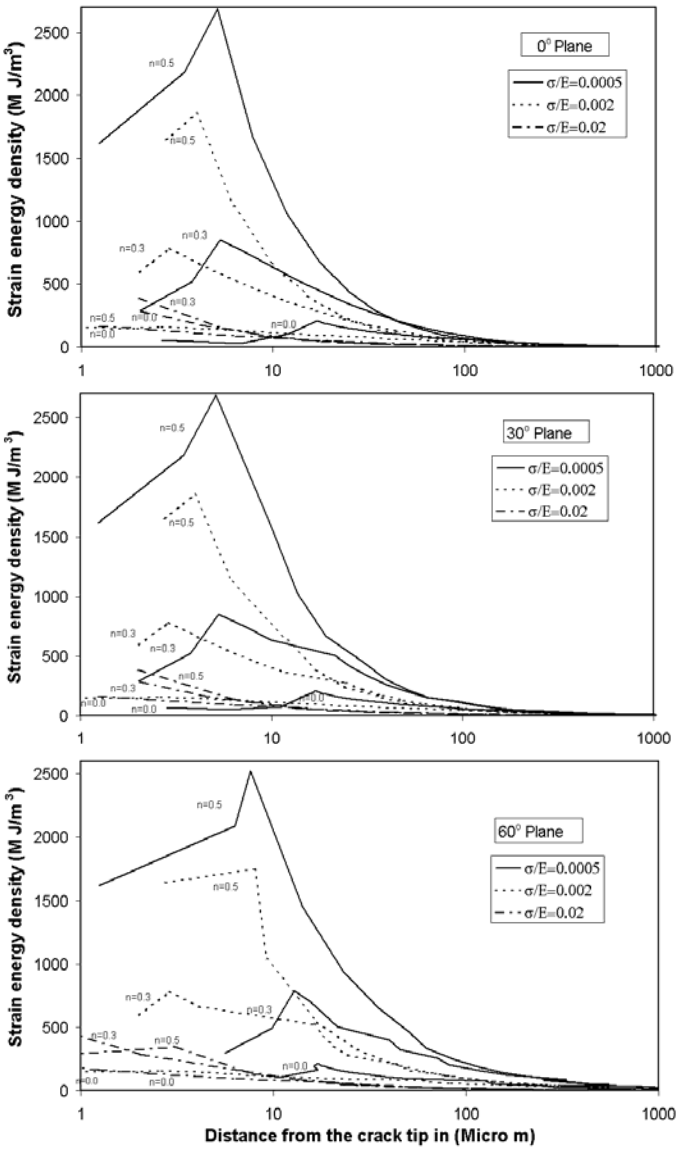

Figure 7 : Plastic strain energy distribution at the crack tip for materials with varying σ_0 / E and n on 0^o, 30^o and 60^o planes

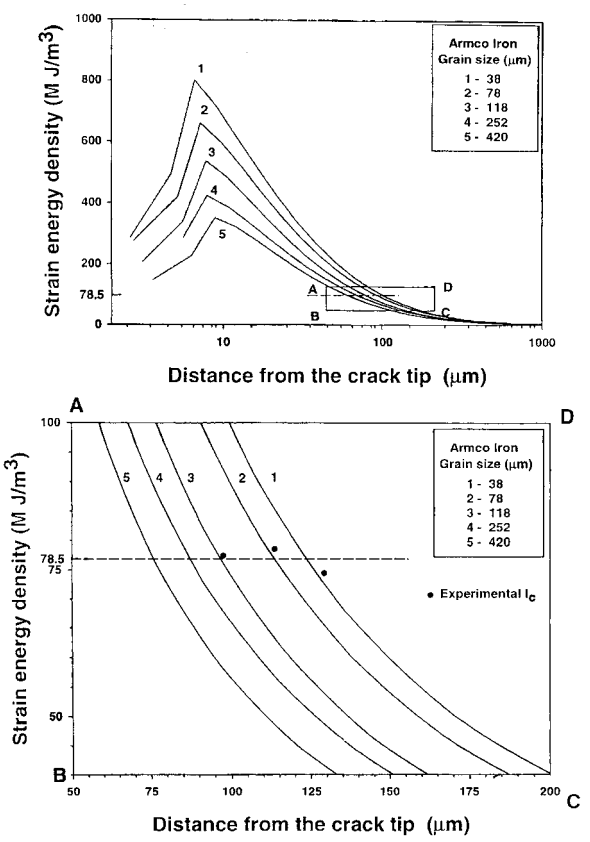

Figure 8 : Plastic strain energy distribution for Armco iron, computed using FEM (a) entire plot, and (b) magnified view of the rectangular zone ABCD of Figure 8a

different grain sizes is shown in Figure 8a. Denser mesh configurations did not improve the value of ϕ at the characteristic distances, that is, the crack tip mesh sensitivity nearly vanishes at about 100 microns. This is expected since ϕ varies inversely with r. The value of ϕ reaches a maximum close to the crack tip ($\sim 10\mu$m)p and falls off steeply with the distance from the crack tip. Although the actual deformation zone spreads up to nearly $1000\mu m$, it can be seen that the pronounced deformation is restricted to a distance of only about 100 microns. A quantitative delineation of the process zone is not possible unless a cut off value is imposed for ϕ. Let us suppose, the strain energy density (ϕ) exceeds a critical value (ϕ_c) in the entire process zone. Then, the dimension of the process zone (l_c) can be determined, as shown in Figure 8a, using,

$$\phi\,(l_c) \;=\; \phi_c \tag{5}$$

The magnified view of the rectangular zone ABCD of Figure 8a is shown in Figure 8b. The experimentally determined l_c values for three different Armco iron materials, of varied grain size, are first plotted on the strain energy density (ϕ) variation in Figure 8b. Since the points fall in a narrow band of about $\pm 2\%$, a constant ϕ_c is fitted in Figure 8b. For $\phi_c \approx 78.5$ M Joules / m^3, the values of $l_c$computed using equation (5) and the experimentally observed ones for Armco iron of different grain sizes in Figure 8 match satisfactorily.

For a power law material,

$$\phi_c = \int_0^{\varepsilon_c} K\varepsilon^n d\varepsilon = \frac{K\varepsilon_c^{n+1}}{n+1} \tag{6}$$

For $\phi_c \approx 78.5$ M Joules / m^3 in equation (6), the resulting ε_c values for Armco iron materials of different grain sizes varybetween 0.21 to 0.24. These values are roughly the same as the void nucleation strain values in such materials. This is reasonable since the necking instability strain, which is the strain hardening exponent (n) itself, varies between 0.25 and 0.3 in these cases [Srinivas et al. (1991)]. This leads us to understand the 'process zone' as the zone of intense plastic deformation with a high possibility of void nucleation, which is consistent with the earlier propositions.

4 J_{IC} - l_C - $CTOD_C$ relationship

4.1 J_{IC} - l_C relationship

Srinivas et al. (1994), in an attempt to relate J_{IC} to l_c, considered the strain energy densities pertaining to the process and the HRR zones, multiplied them with respective sizes of the zones and expressed J_{IC} as a function of the sum of these two energy-length products. Implicitly, the energy densities have been assumed to be uniform in the respective zones but this affected the accuracy. In this follow-up study, the area under the strain energy density curves shown in Figure 8a was computed up to the boundary of the process zone and was plotted as a function of the respective J_{IC} values. This plot is shown in Figure 9. The correlation is almost linear, which means

$$J_{IC} \;\approx\; \kappa \int_0^{l_c} \phi\, dr \tag{7}$$

A point to note is that the integration limits include the instability zone in the vicinity of the crack tip, which is

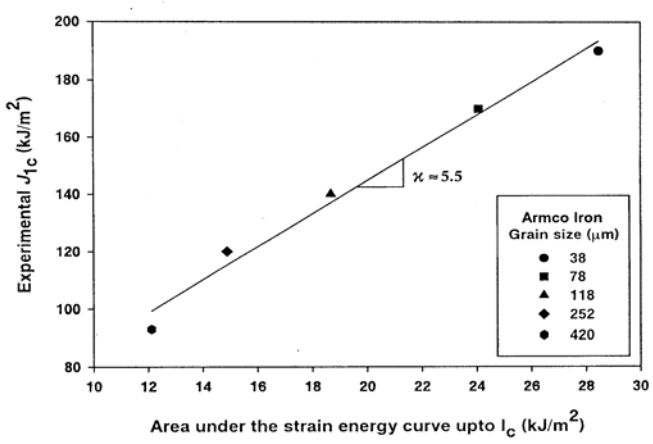

Figure 9 : J_{IC} vs area under the strain energy density (ϕ) curves (in Figure 8a) up to lc.

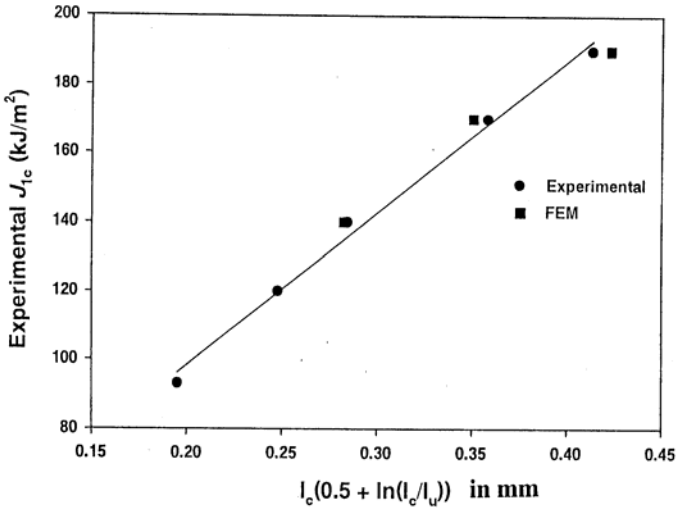

Figure 10 : Validation of the J_{IC}–lc relationship (equation 9).

an order of magnitude smaller than the process zone. A discussion on the instability zone is given in the following section.

According to the HRR equation [Hutchinson (1968a,b); Rice(1968)] the plastic strain (ε follows $(1/r)^{(1/1+n)}$ variation with the distance (r) from the crack tip and this has been experimentally verified by Kwai S. Chan (1990) for stationary cracks. The plastic strain $\varepsilon \propto (1/r)^{(1/n+1)}$ and $\phi_c \propto \varepsilon^{n+1}$ as in equation (6) lead to $\phi \propto 1/r$. On the other hand, in the region of unloading, '$\phi \propto r$' is assumed based on the numerically obtained variation in the unloading region (Figure 8a) and the variation of ϕ is approximated as the line joining ϕ_{max} with the origin (0,0). Since, $\phi(l_c) = \phi_c$ as in equation (5), it can be shown that,

$$\left.\begin{array}{ll} \phi = \frac{\phi_c l_c}{r} & for \quad r \geq l_u \\ \approx \frac{\phi_c l_c r}{l_u^2} & for \quad r \leq l_u \end{array}\right\} \tag{8}$$

where l_u is the dimension of the zone of unloading that occurs due to blunting and $\phi(l_c) = \phi_{max}$. The error introduced by the linear approximation in the unloading region is insignificant and the results are only mildly sensitive to the magnitude of l_u. Finally, substituting equation (8) in equation (7) and simplifying, we get a J_{IC} - l_C relationship,

$$J_{1C} \approx \kappa \, \phi_c \, l_c \left(\frac{1}{2} + \ln \frac{l_c}{l_u}\right) \tag{9}$$

To verify the above equation, J_{IC} was plottedas a function of l_c (0.5+ln (l_c/l_u)) using the values obtained in the numerical experiments (FEM) and the experimentally measured ones by Srinivas et al. (1994) in Figure10. Since experimental values are not available for $l_{u,}$, FEM generated values were used. The linear relationship exhibited in Figure 10 confirms the validity of equation (9) and the constant works out to $\kappa \approx 5.5$. In the present study, κ was found to be independent of the grain size of Armco iron.

The emphasis of the plot in Figure 10 is the linear variation between $J_{IC}$and the function l_C (0.5 + ln (l_C /l_U)), and not the correlation between the FEM results and the experimental ones. Naturally, the experimental and the FEM data would agree because the FEM study is a simulation of the experiment and the material data for the FEM study were extracted from the experimental results only. It is at best useful in validating the FEM methodology employed. On the other hand, the linearity is interesting and it supports equation 9 as well. Experimental data on $J_{IC}$and l_c used in Figure 10 are independent of the FEM as well as the analytical models and therefore not influenced by the value ϕ_C= 78.5 MJ/m^3. The size of the unloading region (l_u), although picked from the FEM results, does not significantly affect the results due to the logarithmic variation.

4.2 J_C- $CTOD_C$ Relationship

The relationship between J and CTOD was experimentally studied for a variety of materials, particularly in the

context of experimental determination of J_{IC} using the stretch zone width (SZW) method, by a number of investigators. The value of J has been found to vary linearly with CTOD and this linearity is described as the *blunting line*. A majority of the above studies focussed their attention on the slope of the blunting line, that is 'mσ' of equation (3). 'σ' is a stress measure and 'm' is understood to be a constant. In one of our recent investigations Suresh et al. (1999), the slope of the blunting line was studied for a variety of materials using numerical (FEM) experiments and the results were validated.

For the commonly used stress measures, such as, $\sigma = \sigma_y$ or $\sigma = (\sigma_y + \sigma_u)/2$,, m turns out to be material dependent. Here σ_y and σ_u represent yield and ultimate strength respectively. Suresh et al. (1999) found that the following stress measure, an integral average of the true stress, makes 'm' a nearly material independent parameter:

$$\sigma \;=\; \sigma^* \;=\; \frac{\int_0^{\varepsilon_l} \sigma \; d\varepsilon}{\int_0^{\varepsilon_l} d\varepsilon} \tag{10}$$

where ε_l is a limiting strain. For a specific case like power-law variation, the limiting strain was assumed to be the strain hardening exponent (n) itself, as consider instability sets in beyond this strain in a tensile specimen. In this case, the stress measure becomes,

$$\sigma^* \;=\; \frac{K\, n^n}{n+1} \tag{11}$$

The use of this stress measure markedly reduces the range of m to $1.1 < m < 1.4$ for a wide variety of materials and the average m (referred to here as m^*) is about 1.25. The J_C-$CTOD_C$ relationship therefore becomes,

$$J_{IC} \;=\; m^* \sigma^* \, CTOD_{IC} \tag{12}$$

4.3 l_c - $CTOD_c$ relationship

The J_{IC} - l_c relationship as in equation (9) and the J_{IC} - $CTOD_C$ relationship as in equation (12) can be combined to provide an equation relating the characteristic distance (l_c) and the critical crack tip opening displacement ($CTOD_c$) as

$$CTOD_C \;\approx\; \left(\frac{\kappa}{m^*}\right) \left(\frac{\phi_c}{\sigma^*}\right) \; l_c \left(\frac{1}{2} + \ln \frac{l_c}{l_u}\right) \tag{13}$$

In equation (13), ϕ_c / σ^* gcan be assumed to be roughly the void nucleation strain (ε_c) itself, $\kappa / m^* \approx 4$ since $\kappa \approx 5.5$ as in Figure 9 and $m^* \approx 1.25$ ($1.1 < m^* < 1.4$) given in Suresh et al. (1999). Therefore, equation (13) reduces to,

$$CTOD_C \;\approx\; 4 \varepsilon_c l_c \left(\frac{1}{2} + \ln \frac{l_c}{l_u}\right) \tag{14}$$

5 Discussion

Let us consider the three queries pertaining to l_c raised in section 1. It clearly emerges that l_c is not just an adjustable length-parameter but one that can be regarded as the dimension of the intense plastic zone or what is termed as the process zone by earlier investigators. Based on the present numerical results, it can be concluded that in the entire process zone the strain energy density exceeds a critical value required for void nucleation. This value can be used as a cut-off value to delineate the zone.

The present analysis on characteristic distance is continuum based and the results agree satisfactorily with the experimental results of Srinivas et al. (1994) for Armco iron, a relatively 'clean' material. In this FEM study introducing voids or particles in the vicinity of the crack tip was therefore avoided. Rather, a crack-tip blunting was analysed in a 'clean' continuum and a consideration of the influence of voids or particles was deferred. Nevertheless, these results are discussed in relation to those based on micro structural considerations for a preliminary understanding of the fracture process.

Ritchie and Thompson (1985) expressed l_c as an integral multiple of grain size whereas Knott (1980) related it to the integral multiple of inter-particle distance, both essentially considering void nucleation at their assumed preferential sites. Tsann Lin (1986) analysed the effect of grain size as well as particle spacing on fracture toughness. Srinivas et al. (1994) found $l_c$to be smaller than the grain-size in some of their experimental observations and attributed the void formation to slip-line intersection. It is well established that grain boundaries, particle-matrix interfaces or slip intersections provide the most probable sites for void nucleation. Therefore, one would expect this type of void to nucleate at the potential site nearest to the crack tip since the effective plastic strain is large near the crack tip and it decreases exponentially with distance from the crack tip. However, the experimental evidence shows that the fracture initiation related void need

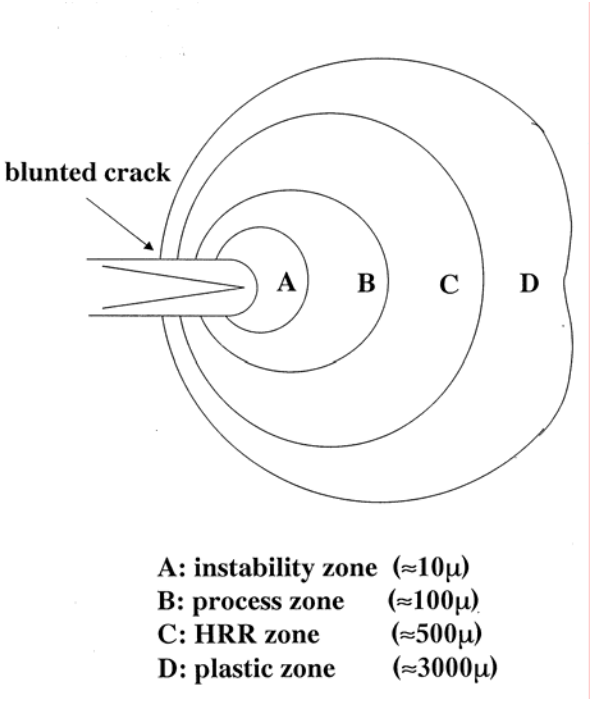

Figure 11 : Delineation of zone of deformation in the crack tip environment (Armco iron).

not nucleate at the nearest site. This aspect leads us to follow the earlier researchers [Knott (1980); Hancock (1980); Mackenzie et al. (1977)], and recognise the importance of void growth in addition to void nucleation. As pointed out by these investigators, although the support for void nucleation by plastic strain decreases with the distance from the crack tip, the hydrostatic stress aiding void growth increases with the distance. In Figure 5(b), the variation of hydrostatic stress with the distance from the crack tip has been plotted for materials with varying σ_0/E and n. The plot corresponding to σ_0/E = 0.0005 and n = 0.3 would be the closest to the case of Armco iron for which l_c has been measured to be about 100 μm. From this plot it is clear that *within the process zone* for this material, the edge of the process zone (l_c from the crack tip) would experience the highest value of the hydrostatic stress, the fact that provides a means of understanding as to why the fracture initiating void occurs at the characteristic distance (l_c) from the crack tip.

The initiation of the final fracture involving coalescence of the 'stable' void with the crack tip has been here dealt with in terms of strain energy density (ϕ) which encompasses the effects of stress and strain. While ϕ exceeds a critical value ϕ_c for void nucleation throughout the process zone, the cumulative value of ϕ represented by the area under the ϕ-r plot (Figure 8a) up to the edge of the process zone is shown to be a measure of J_{IC}. Interestingly, the value of ϕ_c = 78.5 MJoules/m^{3}fitted in Figure 8b, for which the computed and experimentally measured l_c of Srinivas et al. (1984) match, the corresponding ε_c values obtainable using equation (6) for Armco iron of varying grain size fall between 0.21-0.24, roughly the same as the void nucleation strain in Armco iron by Srinivas et al. (1991).

Based on the above, it can be stated that l_c , the dimension of the process zone, is indeed an experimentally measurable parameter. Such an attempt was earlier made by Srinivas et al. (1984) who measured the distance between the crack tip and what they referred to as an *appropriate void* ahead of the crack tip in the crack plane. They deliberately discarded the void formed very close ($\sim$10μm) to the crack tip and chose a near-spherical void formed at a distance. *In the present study, the crack tip void is recognised as the instability related one and the void formed away from it as the one corresponding to l_c.*

For Armco iron as in Srinivas et al. (1994), Figure 11 depicts the delineation of the instability zone in comparison with the other zones recognised in the earlier studies. Although l_c is experimentally measurable, any accurate determination of J_{IC} using l_c is still not possible because of, on the one hand, the uncertainties in equation (2) and on the other, due to the need to ascertain wider applicability of equation (9). This is in contrast with the J_{IC} - $CTOD_{1C}$relationship (equation 12) that has matured as a reliable equation using which J_{IC} can be established using the stretch zone width method [Suresh et al. (1999)]. Nevertheless, equation (2) and equation (9) throw helpful light on crack tip blunting mechanics.

6 Conclusions

Finite Element Method, based on a large deformation framework, has been used to simulate crack tip blunting prior to ductile fracture. The aim was to understand the experimental observations in regard to voids formed at a distance from the crack tip, referred to as the characteristic distance (l_c). In the present continuum study, the focus of attention was on the observations reported in Srinivas et al. (1994) pertaining to nominally particle free Armco iron. The following points emerge:

1. The analysis suggests that the size of the zone of

intense plastic deformation, the process zone ahead of the crack tip, delineated by a critical strain energy density (ϕ_c), compares well with the experimentally measured l_c. This ϕ_c value roughly correspond to the plastic strain required for void nucleation.

2. It emerges from the present study that, of the voids observed by Srinivas et al. (1994) in interrupted CT tests on Armco iron, those voids close to the crack tip can be regarded as instability voids and the void formed away from the crack tip as the one corresponding to l_c,the dimension of the process zone.

3. The hydrostatic stress (σ_m), responsible for void growth, increases within the process zone as seen in Figure 5(b). Therefore, $\sigma_m$has its highest value at the edge of the process zone that is identified as the site for the void associated with l_c.

4. The integral of the variation of ϕ from the crack tip to the void site at l_c is found to be linearly related to J_{IC} (equation 9). Combining equation (9) with the relationship between J_{IC} and the crack tip opening displacement ($CTOD_C$), proposed by Suresh et al. (1999), a relation has been arrived at connecting l_c and CTODc.

Acknowledgement: We thank Dr. M Srinivas, Dr. S.V. Kamat and Dr. Malakondiah of DMRL for valuable discussions and Shri R.K.V.Suresh of Osmania University for his assistance in carrying out the numerical work. The support of DRDO is also acknowledged with thanks.

One of the authors (PRR) records his gratefulness to the Indian Space Research Organization for the award of a Professorship.

References

ASTM standard E 1152-87 (1987): Standard Test Method for determining J-R curves, *Annual Book of ASTM standards Philadelphia*, pp. 814-818.

ASTM standard E 813-81 (1986): Standard test method for J_{IC}, A measure of fracture toughness, *Annual Book of ASTM standards Philadelphia,* pp. 768-782.

Begley, J. A.; Landes, J. D. (1972): The J-integral as a fracture criterion, *American Society for Testing and Materials ASTM STP 514 Philadelphia,* pp. 1-20.

Chan, Kwai S. (1990): *Metallurgical Transactions A* (21A), pp. 69-86.

Gao, X.; Faleskog, J.; Shih, C. F.; Dodds, Jr. R. H. (1998): Ductile Tearing in Part-Through Cracks: Experiments and Cell-Model Predictions, *Engineering Fracture Mechanics* 59 (6), pp. 761-777.

Green, G.; Knott, J. F. (1976): *Journal of Engineering Material and Technologgy* 1, pp. 37-46.

Gullerud, A. S.; Gao, Xiaosheng; Dodds, Jr. R. H.; Haj-Ali, R. (2000): Simulation of Ductile Crack Growth Using Computational Cell: Numerical Aspects, *Engineering Fracture Mechanics* 66, pp. 65-92.

Hancock, J. W. (1992): *Topics in Fracture and Fatigue*, Springer-Verlag Publishers, New York, pp. 99-144.

Hancock, J. W.; Cowling, M. J. (1980): *Metal Sciences* 4, pp. 293-304.

Hutchinson, J. W. (1968a): Singular Behaviour at the end of a tensile crack in a hardening material, *Journal of Mechanics and Physics of Solids* 16, pp. 13-31.

Hutchinson, J. W. (1968b), Plastic stress and strain fields at a crack tip, *Journal of Mechanics and Physics of Solids* 16, pp. 337-347.

Jackson, J. H. ; Kobayashi, A. S; Atluri, S. N. (2004): A Three Dimensional Numerical Investigation of the T* integral along a curved crack front, CMES: Computer Modelling in Engineering Sciences Vol.6, No.1, pp 17-30.

Knott, J. F. (1980): *Metal Sciences* 6, pp. 327-336.

Landes, J. D.; Begley J. A. (1972): The effect of specimen geometry on J_{IC}, *American Society for Testing and Materials,ASTM STP 514 Philadelphia,* pp. 24 -39.

Liebowitz, H.; Moyer, E. T. (1989), Finite element methods in fracture mechanics, *Computers and Structures* 31, pp. 1-9.

Lin, T. (1986): *Acta Metallurgica* 34, pp. 2205-2216.

Mackenzie, A.C.; Hancock, J. W.; Brown D. K. (1977): *Engineering Fracture Mechanics* 9, pp. 167-188.

McMeeking, R. M. (1977): Finite deformation analysis of crack tip opening in elastic-plastic materials and implications for fracture, *Journal of Mechanics and Physics of Solids* 25, pp. 357-381.

Meguid, S. A. (1989): *Engineering Fracture Mechanics*, *Elsevier Applied Science, London and New York* , pp. 233.

Ortiz, M.; Leroy, Y.; Needleman, A. (1987): *Computer Methods in Applied Mechanics and Engineering* 61, pp. 189-201.

Ramakrishnan, N.; Atluri, S. N. (1994a): *International Journal of Plasticity* 10(5), pp. 499-534.

Ramakrishnan, N.; Atluri, S. N. (1994b), *Mechanics of Materials* 17, pp. 307-317.

Ramakrishnan, N.; Singh, K. M.; Suresh, R. K. V.; Srinivasan, N. (1999): An algorithm based on Total-Elastic-Incremental-Plastic strain for large deformation plasticity, *Journal of Material Processing Technology* 86, pp. 190-199.

Rice, J. R. (1968): A path independent integral and the approximate analysis of strain concentrations by notches and cracks, *Journal of Applied Mechanics, Transaction ASME* 35, pp. 379-386.

Rice, J. R.; Johnson, M. A.; Kanninen, M. In; Adler, W. G.; Rosenfield, A. R.; Jaffee, J. I. (1970): *Inelastic behaviour of solids*, McGraw-Hill Publishers, New York and London 1970 (eds.), pp. 641-672.

Rice, J. R.; Rosengren, G. F. (1968): Plane strain deformation near a crack tip in a power-law hardening material, *Journal of Mechanics and Physics of Solids* 16, pp. 1-12.

Ritchie, R. O.; Thompson, A. W. (1985): *Metallurgical Transactions A* 16(A), pp. 233-248.

Schmitt, W.; Hollstein, T. (1985): Numerical evaluation of crack tip opening displacements: 2D and 3D applications, *Proceeding of the workshop on the CTOD methodology* 3.

Shih, C. F. (1981): Relationships between the J-integral and the crack opening displacement for stationary and extending cracks, *Journal of Mechanics and Physics of Solids* 29, pp. 305-381.

Srinivas, M.; Malakondiah, G.; Armstrong, R. W.; Rama Rao, P. (1991): *Acta Metallurgica* 39(5), pp. 807-816.

Srinivas, M.; Sundararajan, G.; Malakondaiah, G.; Rama Rao, P. (1994): An analysis of ductile fracture initiation toughness in iron, its binary alloys and nickle, *Proceeding of Royal Society, London A* 447, pp. 237-251.

Suresh, R. K. V.; Ramakrishnan, N.; Srinivas, M.; Rama Rao, P. (1999): On the Determination of J_{IC}Using the Stretch Zone with Method, *Journal of Testing and Evaluation* 27(3), pp. 211-217.

Tchouikov, S.; Nishioka, T.; Fujimoto, T. (2004): Numerical Prediction of Dynamically Propagating and Branching Cracks Using Moving Finite Element Method, CMC: Computers, Materials and Continua, Vol. 1, No.2, pp. 191-204.

Tracey, D. M. (1976): Finite element solutions for crack-tip behaviour in small-scale yielding, *Journal of Engineering Materials and Technology (Transaction ASME)* 98, pp. 146-151.

Tsamaphyros, G.; Glannakopoulos, A. E. (1989): *Engineering Fracture Mechanics* 32, pp. 515-522.

Tvergaard, V.; Hutchinson, J. W. (1994): *Journal of Mechanics and Physics of Solids* 31, pp. 823-836.

Warren, M.; Garrison Jr. (1984): *Scripta Materialia* 18, pp. 583-586.

Wilsdorf, H.G.F. (1983): *Material Science and Engineering* 59, pp. 1-39.

Zhang, Z. L.; Thaulow, C; Odegard, J. (2000): A Complete Gurson model Approach for Ductile Fracture, *Engineering Fracture Mechanics* 67, pp. 155-168.